Proceedings of the ASME 2023
International Mechanical Engineering Congress and Exposition
IMECE2023
October 29-November 2, 2023, New Orleans, Louisiana

IMECE2023-113952

FINITE ELEMENT SIMULATION OF THE EFFECT OF THE SECTIONS OF A SOLAR AIR HEAT EXCHANGER

Tiwaloluwa Olukeye
MSc., Mechanical Engineering
Washington, D.C.

Samba Gaye
PhD., Mechanical Engineering
Washington, D.C.

Ali Alshweiki
MSc., Mechanical Engineering
Washington, D.C.

Pawan Tyagi
Professor, Mechanical Engineering
Washington, D.C.

ABSTRACT

Whether your home uses a stove, boiler, or heat pump for its heating needs, they almost always have one thing in common: they require fossil fuels to operate. Given that fossil fuel prices will continue to rise and eventually run out, alternatives are urgently needed. With the ongoing yet gradual transition, one of the environmentally friendly options is solar energy – which is renewable. The solar air heater is one of the essential devices which converts solar energy into thermal energy. This paper reports an experimental analysis of the performance characteristics of sectioning a pumpless solar room air heater using ANSYS Fluent Software, a CFD simulation package that uses applied mathematics to numerically solve a wide variety of mechanical problems – such as heat – and model fluid flow situations. Dimension optimization regarding the section lengths (or distance between features) and the head loss measured was used to improve thermal performance. During the CFD investigation, the design's influence (sectioning of the pipe at varied lengths with respect to head loss) and the Reynolds number on the process of stream aerodynamics and heat exchange were acknowledged. The predicted results were compared with the experimental observations, where the heat-transfer measurements showed a linear relationship between temperature and distance between the turbulators, even as they increased as the other increased.

Keywords: Solar collectors, solar air tubes, computational fluid dynamics (CFD)

1. INTRODUCTION

Energy, being a critical aspect of everyday life, as well as the basis for sustainable living, is known to have a yearly increment in its usage. Majority of the energy needs are being achieved from fossil fuels, and with the costs of such fuels always on the rise, there is a pressing need for other choices to be explored. In eliminating the drawbacks associated with these fuels (such as coal and crude oil), a lot of research work has been carried out in the renewable energy sector. Renewable energy, commonly known as clean or sustainable energy, stems from natural sources which can be replenished, and as such, will eventually play a significant role in the decarbonization of the earth's energy systems in the future. Decreasing environmental pollution is arguably the most important advantage of renewable energy systems. Even as there is a variety of renewable sources such as wind, geothermal, hydroelectric, etc., solar energy is the cleanest and most abundant renewable energy source available (Singh & Singh, 2018).

According to U.S Department of Energy, the extent of sunlight which hits earth's surface in just under two hours is enough to handle the entire world's energy consumption for a full year. Although it is believed that the application of solar energy in buildings began as far back as Socrates (470 – 390 BCE), as well as Archimedes (whose application of solar energy was during combat with the Roman army in 212 BCE where he made use of a concave metallic mirror), Bernard Foret Belidor (1697 – 1761) is the individual known to have the earliest documented application of solar energy, which has been available since the 18th century. Solar houses gained popularity during the early 20th century even as designers developed methods and ways of taking advantage of the sunlight during winter by using large south-facing windows (Goel et al., 2021).

There are various methods involved in harnessing solar energy used for heating applications. However, the most efficient and effective, yet simplest way of utilizing such energy is by converting it to thermal energy using solar collectors (Varun et al., 2007). A solar collector is a device used for collecting solar radiation and transferring the energy to a particular fluid passing in contact with it (the fluid can either be air or water, depending on the application target). There are two main types of solar

collectors, namely: concentrating and non-concentrating. Consisting of concave reflecting surfaces, the concentrating solar collector diverts and directs solar radiation to a smaller receiving region/area. The interceptor area is bigger than the receptor area. Through this process, the radiative flux is increased. Alternatively, as the name suggests, the non-concentrating solar collector does not concentrate its focus on a particular area; it instead has the same area for the interception and absorption of the sun's radiation (Kalogirou, 2004). The concentrating solar collector can further be divided into two types, namely: the line focus solar collector (LFSC) – which comprises the parabolic trough – and the point focus solar collector (PFSC), which comprises the parabolic dish and the parabolic tower. On the other hand, the non-concentrating solar collector is sub-divided into the flat plate solar collector (FPC) and the evacuated tube solar collector (ETSC).

Even though FPCs are the mostly used solar collectors due to their minimal cost of maintenance and design simplicity, they otherwise have relatively low efficiency primarily due to the heat lost through convection (the glass cover) from the collector plate. There is a noticeable change in performance of FPCs during the cloudy or windy days, even as they are mainly designed for warmer climates. Weather plays a huge role in their functionality, efficiency and effectiveness, and as such, there is always the risk of system failure caused by the distortion or the deformation of the internal materials. On the contrary, the presence of a vacuum in the ETSC helps curtail the convection heat loss, by this means increasing efficiency. They have exceptional thermal performance with ease of movement and are suitable for harsh temperatures. A typical ETSC consists of parallel glass pipes comprised of an outer tube and an inner one. The inner tube has some sort of coating on it (a material with high radiation absorptivity), which clearly distinguishes itself from the outer tube – which is transparent. When light is incident upon the ETSC, it passes through the outer tube and is absorbed by the inner tube. The purpose of the vacuum is to keep the absorbed heat within the inner tube, even as it gets heated due to the selective coating (Essa & Mostafa, 2017), (Sabiha et al., 2015).

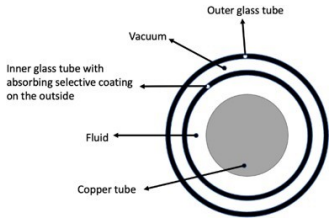

FIGURE 1: CROSS-SECTION OF A SOLAR AIR HEATER TUBE.

The two main types of configurations associated with using ETSC are the solar water heater (SWH) and the solar air heater (SAH). When compared with the SWH, the SAH has a disadvantage of low heat transfer capability. However, its cost-effectiveness and simplicity give it the edge, thus making it the better choice when it comes to longevity. Unlike water, air cannot freeze, neither can corrosion of any form occur in/on the collector. The energy (or heat) absorbed by the transfer fluid can then be used for domestic purposes like water heating and space heating, or even cooling (Goel et al., 2021). After A.G. Eneas powered a water pump at a California farm through a 10-meter focusing collector using 1788 mirrors, many variations and innovative ideas of applying the solar collectors for heating the working fluid powering mechanical equipment have been designed and produced over the past century (Kalogirou, 2004).

Researchers over the years have made design variations of such type of a system. Analyzing the thermal performance of the SAH is a prerequisite for making an efficient and effective design for economic viability. For better understanding, a standard SAH is studied for the thermal analysis. With a technical perspective in view, it is essential that the system is designed to be capable of supplying year-round power, or at least capable of providing required energy output at the time of demand (Saxena et al., 2015). Recall, the thermal efficiency of SAH is relatively low compared to SWH due to its low heat capacity. However, augmenting the heat transfer coefficient is one way of making the SAH economically viable. This can be achieved through passive techniques (no external energy supply), active techniques (presence of external energy supply), or a blend of both techniques. The passive techniques can come in different methods such as expanding the heat transfer area using fins (extended surfaces), generating turbulence at the heat-transferring surface (rough surface), using coiled tubes, using additives for gases and liquids, etc. (Varun et al., 2007).

FIGURE 2: A STANDARD ETSC SOLAR AIR HEATER TUBE.

One of the most efficient and commonly used passive methods for improving thermal performance and heat transfer rate is using turbulator devices. Turbulators are artificial flow alteration devices which create some sort of turbulence thereby modifying the fluid stream (Kumar et al., 2016). They are easy to fabricate and operate, and they generally have relatively low cost of maintenance. There have been various design modifications and flow factors used over the years by researchers for experimental study. In 2010, Kongkaitpaiboon and the team carried out an investigation using circular-ring turbulators (CRT) and perforated conical-ring (PCR) on the heat transfer and fluid flow friction in a solar air heater tube (Kongkaitpaiboon et al., 2010a), (Kongkaitpaiboon et al., 2010b). In another study on enhancing heat transfer through turbulence, (Kumar et al., 2016)

experimented using solid hollow circular disks (SHCD) turbulators.

Thermal Performance of FPC

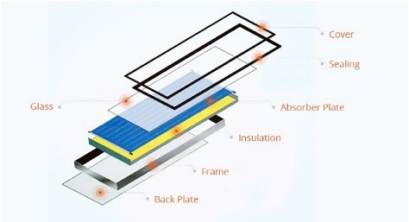

FIGURE 3: FLAT PLATE SOLAR THERMAL HEATER.

Hottel-Whillier is a well-known mathematical model for thermal analysis FPCs; it measures the energy gain of the flat plate solar collectors. Thermal performance of a flat plate solar air heater can be computed with the help of the Hottel–Whillier–Bliss equation:

$$Q_u = A_C F_R[(G_T(\tau\alpha) - U_L(T_i - T_a))]$$

Where:

G_T = the incident solar flux
F_R = the heat removal factor
A_C = the collector area
U_L = the total heat loss coefficient
τ = the effective transmittance of the cover
α = absorbance coefficient of the collector
T_a = the ambient temperature
T_i = the fluid inlet temperature

Thermal Performance of ETSC

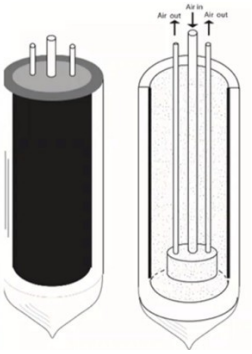

FIGURE 4: EVACUATED TUBE SOLAR THERMAL HEATER.

Sunlight is incident on the outer layer of the evacuated glass tube. A fraction of the radiation is absorbed, another fraction is reflected back into the environment, while majority of it is transmitted to the next layer of glass tube. To calculate the incidence solar radiation flux value, the following formula is used:

$$G\alpha_{sun} = \alpha_{low\ temp}\ \sigma\ (T^4 - T^4_{surr}) \quad (1)$$

The total incident energy available on the surface is:

$$G \times \text{Aperture Area} \quad (2)$$

With the formula above, the outer tube's temperature is obtained, and can then be used to calculate the temperature of the inner glass tube. A vacuum acts as the separation between the two glass tubes, and there is an assumption that only transmission energy takes place from the top layer.

$$Energy_{trans} = \tau \times \text{Energy Incident} \quad (3)$$

2. MATERIALS AND METHODS

Under normal conditions, the total energy per mass unit in a given point in a fluid comprises three main energy types: potential, kinetic and pressure. Here, only deductions of the heat-transfer enhancement efficiency through head loss between features will be discussed.

In this numerical study, the tube and the turbulators were modelled using ANSYS Fluent Software for investigating the thermal performance. The amount of solar radiation was constant, as well as its direction. The transparency of the outer tube, as well as the coating for the inner tube were both considered.

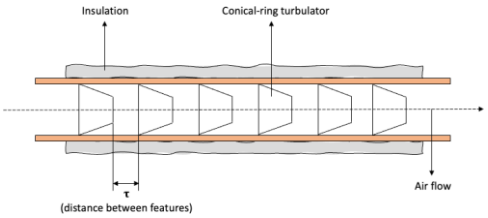

FIGURE 5:CROSS-SECTION OF CONICAL-SHAPED TURBULATORS IN COPPER PIPE.

Two concentric glass tubes with dimensions 43.8 mm inner diameter, 46mm outer diameter, and 483 mm length were used. For evaluation purposes, a maximum of two conical ring turbulators were used at any point in the simulation process. The conical-shaped turbulators were made of copper; with 13.7 mm in length, larger diameter of 20 mm, and smaller diameter of 10 mm.

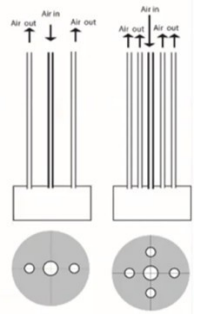

FIGURE 6: CROSS-SECTION SHOWING FLOW OF AIR THROUGH COPPER PIPES.

For the simulation procedure, the turbulators were placed inside the SAH tube, attached to the ends of a copper pipe with a dimension of L = 150 mm for length, D_O = 22 mm for outer diameter, D = 20 mm for inner diameter, and t = 1 mm for pipe thickness. The temperature distribution was also measured along the pipe (at the exit points of the turbulators), and heat loss was minimized through simulated insulation.

In order to establish precise drop in pressure and the heat transfer in the SAH tube, the turbulators in the copper pipe were set at intervals ranging from 10 mm up to 200 mm, alongside a control where no turbulator was present. The CFD predicted results have been compared with the experimental observations. The arrangement of the turbulators is shown in Figure 6.

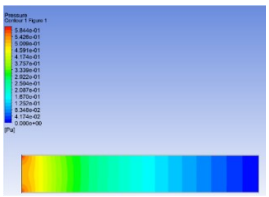

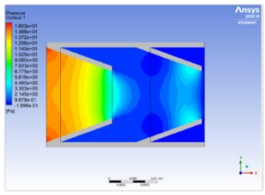

FIGURES 7A & 7B: AIRFLOW-PRESSURE CONTOUR FOR THE PIPE WITH NO FEATURE AND FOR THE PIPE WITH TURBULATORS SET AT A DISTANCE OF 5 MM FROM EACH OTHER.

3. RESULTS AND DISCUSSION

Based on experimental investigation, different results have been obtained for varied sets of turbulator-distance arrangements. Variation of temperature and head loss based on different lengths between features and flow parameters is achieved through simulated experimental data. The data obtained were plotted on graphs depicting the temperature variation and head loss with respect to the distance between the features. The ANSYS software simulated a uniform temperature distribution throughout the pipe. The heat transfer coefficient can be expressed as:

$$h = \frac{!''! \ (\%''\& \ \%\#)}{((\%\$\& \ \%\%)} \quad (4)$$

The heat transfer coefficient (h) can also be stated in terms of Nusselt number, Nu, which is calcuated:

$$Nu = \frac{)*}{+} \quad (5)$$

Where

h = heat trasnfer coefficient
k = thermal conductivity of air
D = diameter

Also, for heating of the fluid (in this case, air), the Nusselt number can be expressed using the equation:

$$Nu = 0.023Re^{0.8}Pr^{0.4} \quad (6)$$

Where

Re = Reynolds Number
Pr = Prandtl Number

Reynolds Number, Re, is a variable that shows the inflow of the working fluid. It is denoted:

$$Re = \frac{\cdot}{\nu} \quad (7)$$

Heat-transfer measurements showed a linear relationship between temperature and distance between the turbulators, even as they increased as the other increased. A simulated velocity of 1m/s was used, and inlet temperature of 15°C was set as the basis for obtaining the outlet temperature, which is defined as:

$$T_{OUT} = T_W + (I_T\text{-}T_W) * e^{\frac{(\&) * 0 * * * \&}{\cdot * *}} \quad (8)$$

Where

T_I = Inlet temperature
T_W = temperature of the water (heating fluid)
ϱ = density
Q = flow rate

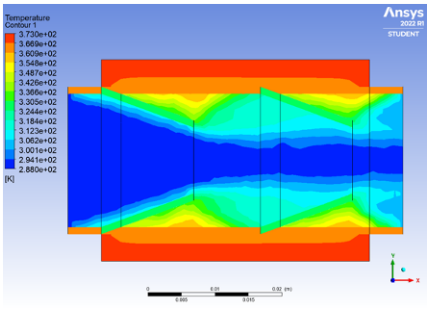

FIGURE 8: THE CONICAL-SHAPED TURBULATORS SET AT A 10 MM DISTANCE.

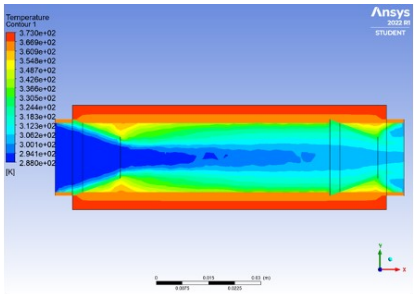

FIGURE 9: THE CONICAL-SHAPED TURBULATORS SET AT A 100 MM DISTANCE.

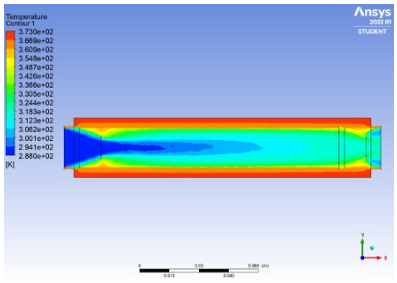

FIGURE 10: THE CONICAL-SHAPED TURBULATORS SET AT A 200 MM DISTANCE.

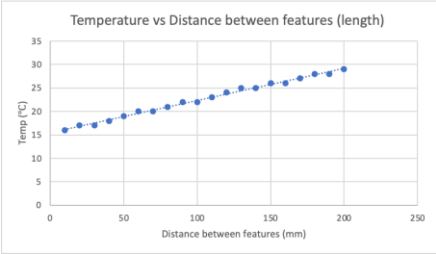

FIGURE 11: GRAPH SHOWING TEMPERATURE VS. DISTANCE BETWEEN THE FEATURES.

However, there was a significant pressure drop caused by the conical-shaped turbulators when compared to the simulation run without the features. The friction head loss is used in the Darcy-Weisbach equation to estimate the pressure drop Δp for a fluid flowing at a velocity V, in a pipe having length L and the hydraulic diameter D, and friction factor f, such that:

$$\Delta p = \frac{102^{+}}{34^{*}} \tag{9}$$

Because flow with a Reynolds number less than 2,100 is termed laminar, and the Reynolds number in this simulation was derived as 1.35E+03, therefore the friction factor for this experimental study was expressed as:

$$f = \frac{56}{78} \tag{10}$$

The experimental investigation indicated that there was a linear relationship between the distance between features and the head loss. This can be seen as plotted on the graph below:

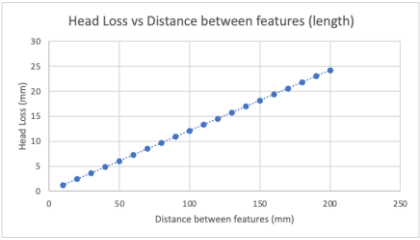

FIGURE 12: GRAPH SHOWING THE RELATIONSHIP BETWEEN THE DISTANCE AND THE HEAD LOSS.

4. CONCLUSION

The simulated convection heat transfer performance of water on air was studied through a horizontal tube with enhancement devices (conical turbulator). This research was performed in varied feature distance arrangements. The results clearly show that increasing the distance between the turbulators influences the head loss, which then influences the heat transfer. Thus, turbulators with smaller distances between each other can be used to enhance heat transfer efficiency.

.

ACKNOWLEDGEMENTS

This paper was prepared under the MECH 500 Research Methods and Technical Communication course taught by Professor Pawan Tyagi in the Fall of 2022. We acknowledge funding support for this course from National Science Foundation-CREST Award (Contract # HRD- 1914751), the Department of Energy/ National Nuclear Security Agency (DE-FOA-0003945), and the NASA MUREP grant (80NSSC19M0196).

REFERENCES

1. Arunkumar, H. S., Karanth, K. V., & Kumar, S. (2020). Review on the design modifications of a solar air heater for improvement in the thermal performance. Sustainable Energy Technologies and Assessments, 39, 100685.
2. Yadav, A. S., & Bhagoria, J. L. (2013). Heat transfer and fluid flow analysis of solar air heater: A review of CFD approach. Renewable and Sustainable Energy Reviews, 23, 60-79.
3. Saxena, A., Srivastava, G., & Tirth, V. (2015). Design and thermal performance evaluation of a novel solar air heater. Renewable Energy, 77, 501-511.
4. Kumar, A., Chamoli, S., & Kumar, M. (2016). Experimental investigation on thermal performance and fluid flow characteristics in heat exchanger tube with solid hollow circular disk inserts. Applied Thermal Engineering, 100, 227-236.
5. Anvari, A. R., Lotfi, R., Rashidi, A. M., & Sattari, S. (2011). Experimental research on heat transfer of water in tubes with conical ring inserts in transient regime. International Communications in Heat and Mass Transfer, 38(5), 668-671.
6. Yakut, K., Sahin, B., & Canbazoglu, S. (2004). Performance and flow-induced vibration characteristics for conical-ring turbulators. Applied Energy, 79(1), 65-76.
7. Kongkaitpaiboon, V., Nanan, K., & Eiamsa-Ard, S. (2010). Experimental investigation of heat transfer and turbulent flow friction in a tube fitted with perforated conical-rings. International Communications in Heat and Mass Transfer, 37(5), 560-567.
8. Pashchenko, D. I. (2018). ANSYS fluent CFD modeling of solar air-heater thermoaerodynamics. Applied Solar Energy, 54(1), 32-39.
9. Anvari, A. R., Javaherdeh, K., Emami-Meibodi, M., & Rashidi, A. M. (2014). Numerical and experimental investigation of heat transfer behavior in a round tube with the special conical ring inserts. Energy conversion and management, 88, 214-217.
10. Saxena, A., Srivastava, G., & Tirth, V. (2015). Design and thermal performance evaluation of a novel solar air heater. Renewable Energy, 77, 501-511.